

Dynamical Advantages of Scale-Free Networks

Frederick H. Willeboordse*

Department of Physics, The National University of Singapore, Singapore 119260

(Received 14 May 2004; revised manuscript received 12 September 2005; published 13 January 2006)

A dynamical analysis of common network topologies is given and it is reported that a scale-free structure has two vital and distinctive features. First, complex but nevertheless reproducible states exist and, second, single-site induced state switching reminiscent of gene-expression control exists also. This indicates that scale-free networks have key dynamical advantages over other network topologies that could have contributed to their evolutionary success and thus may provide another reason for their prevalence in nature.

DOI: [10.1103/PhysRevLett.96.018702](https://doi.org/10.1103/PhysRevLett.96.018702)

PACS numbers: 89.75.Hc, 05.45.Ra, 89.75.Fb

The discovery of the ubiquity of scale-free networks [1,2] and especially their prevalence in biology has led to many exciting insights into fundamental underlying principles that govern complex systems, and much progress has been made in understanding properties that are more or less direct consequences of the topology [3]. Even so, the network anatomy needs to be complemented by network dynamics as especially biological systems contain large numbers of constituents that have their own dynamics but whose collective actions determine the overall behavior. It is therefore essential to consider the temporal evolution of complex networks [4,5] as was, e.g., recently done by Argollo de Menezes and Barabási in a study of five natural and technological networks [6], or the convergence of duplication graphs to unique attractors as investigated by Raval [7].

Here, the problem of understanding dynamical features is approached differently by placing simple chaotic elements on top of commonly encountered network topologies [8–12]. The overall network behavior is then observed as a function of the structure and of parameters representing the strength of the links and the local nonlinearity. This approach is based on (for complex systems), the generally successful premise that universal features often emerge from fundamental properties such as the network structure, coupling, and local dynamics [13,14].

Usually systems as employed here are referred to as coupled map lattices and stunningly rich phenomenologies have been discovered in many prototype models that powerfully describe unifying underlying principles [15–21]. A further motivating factor is the concept that cell states can be considered as attractors of the complex system formed by the cellular constituents [22]. Consequently, it is of particular interest to study how attractor landscapes are influenced by network topology.

Figure 1 shows the network topologies compared here for the case of 10 or 16 nodes for ease of visibility, though the simulations were carried out for networks with between 50 and 200 nodes. Figure 1(a) shows diffusive links that have been extensively studied by physicists for analyzing the spatiotemporal behavior of high-dimensional chaotic

systems. Nodes were lined up on a circle and first and second nearest neighbors connected. Figure 1(b) shows the hierarchical network that combines a scale-free structure with modularity, albeit in this case at the expense of a random component. Figure 1(c) shows the small-world network based on the topology introduced by Watts and Strogatz to combine local links [as in Fig. 1(a)] with relatively short path lengths to other nodes by adding a number of random links. The network is obtained by adding some random links to Fig. 1(a) (this slightly increases the average degree). Figure 1(d) is the original model of Watts and Strogatz, which again starts with a diffusive topology but then continues by randomly rewiring links (this keeps the average degree constant). Figure 1(e) shows the scale-free networks as introduced by Barabási to model the coexistence of highly connected hubs with less connected nodes as encountered in, e.g., the Internet and intracellular networks. After starting with two linked nodes, the network is grown by preferential attachment. Figure 1(f) shows a random network as described by the random graph theory of Erdős and Rényi (ER-random networks). Nodes were randomly selected and then randomly linked to another node.

For the purpose of the investigation here, given a certain set of parameters, the behavior of the commonly described network topologies like the diffusively or globally coupled

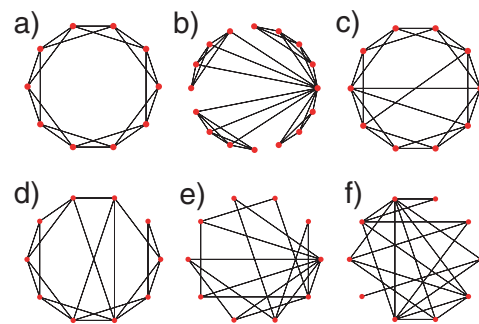


FIG. 1 (color online). Network topologies whose dynamics are compared: (a) diffusive, (b) hierarchical, (c) small-world, (d) Watts-Strogatz, (e) scale-free, and (f) ER-random.

map can be roughly divided into two broad classes when running the simulations many times from random initial conditions: Either there is a very large number of generally similar but clearly nonidentical attractors like the frozen random patterns in the diffusively coupled logistic lattice [23], or there is a small number of usually nearly identical attractors that do not depend on the initial settings such as the wavelike pattern selection attractors again found in the diffusively coupled logistic lattice [24] (a similar distinction can also be made in globally coupled maps by considering the partially ordered and ordered phases [15]).

Defining attractor diversity as the fraction of different attractors that can be obtained when resetting the simulations completely, such that both new random initial conditions and new wirings between the nodes are chosen, and attractor reproducibility as one minus the fraction of different attractors that can be obtained when only restarting the simulation with new random initial conditions but without rewiring the nodes, it follows that topologies like diffusive and global coupling, due to their lack of random connections, can display attractor diversity without attractor reproducibility (frozen random pattern) or attractor reproducibility without attractor diversity (wavelike pattern selection).

In biological and other systems capable of (evolutionary) progress, however, one would need a combination of both diversity and reproducibility. That is to say, there should be a large space of possible arrangements representing system functionality, while a given arrangement should yield reproducible results in that it should not be very sensitive to the environment and allow for only a limited number of different attractors.

To compare attractor diversity and reproducibility, simulations were carried out on the six network topologies shown in Fig. 1 in the following way: a logistic map given by $x_{n+1} = f(x_n) = 1 - \alpha x_n^2$ with x the state variable, n the time, and α the nonlinearity is placed at each node and coupled according to the network topology with a coupling constant ε such that the state of node i at time step $n + 1$ is determined by

$$x_{n+1}^i = (1 - \varepsilon)f(x_n^i) + \frac{\varepsilon}{N_{L(i)}} \sum_{L(i)} f(x_n^{L(i)}), \quad (1)$$

where the sum is over the nodes $L(i)$ linked to node i and $N_{L(i)}$ is total number of nodes linked to i . The logistic map, which has its origins in population dynamics [25] as a simplified model for growth in small populations and inhibition due to overcrowding in large populations, was used to represent the dynamics of a node since it is also an excellent prototype for elements that can display both chaotic and nonchaotic behavior. Consequently, the logistic map is well suited for investigating generic properties of dynamical networks.

The numerical results are obtained from a number of runs N_R where each run r has two parts. In the first part, the diversity D is determined by starting the simulation M times from random initial conditions each time rewiring

the network according to the requirements of the topology. In the second part, the reproducibility R is determined by starting the simulation M times from random initial conditions without rewiring the network. Diversity and reproducibility are then obtained as

$$\text{Diversity } D = \frac{N_A}{M} \quad \text{with rewiring}, \quad (2)$$

$$\text{Reproducibility } R = 1 - \frac{N_A - 1}{M - 1} \quad \text{without rewiring} \quad (3)$$

from the number of attractors, N_A , which is given by

$$N_A = \sum_{k=1}^M \Theta \left(\min_{\substack{j \in [1, N], j \neq i \\ l \in [1, M], l \neq k, m}} \left[\sum_i |y_{i,k} - y_{i+j,l} - \delta| \right] \right), \quad (4)$$

where the matrix y consists of M columns that store a representation of the final states of each simulation. Columns m , which have been found to be fulfill the criterium of being identical to another column, are excluded from further consideration to exclude double counting. The constant δ is a small number (here $\delta = 10^{-4}$ was used) and the sum i is over the column length N (generally this would be number of nodes N_N , however, depending on the method of representing the attractor, e.g., when coarse graining, it can be different). Consequently, the diversity is large when the number of different attractors is large and reproducibility is large when the number of different attractors is small. As for several topologies, there is no natural way to define space; in all simulations, the nodes were ordered by the number of links.

To obtain an overview of the dynamics, for each topology, the parameters were scanned and 50 runs per parameter pair were carried out. The number of different attractors was counted with the help of Eq. (4) by grouping together nodes with an identical number of links and averaging their dynamical variables. That is to say, the elements of the matrix y for run r are given by $y_{N_L, r} = \sum_{N_L, T} x_n^{N_L} / N_L$, where the sum is over all the nodes with a given number of links N_L and over an interval $T[n = \text{transient time} \dots \text{transient time} + 4]$ of four successive time steps since the attractors generally have four temporal phases [17].

The results are depicted in Fig. 2, where it can be seen that scale-free and ER-random topologies appear to combine large reproducibility with high diversity rather regularly, while small-world and Watts-Strogatz networks do so only in a limited way. As can be expected, the diffusive and hierarchical networks yield outcomes near the diagonal. The nonlinearity α was scanned from 1.5 to 1.9 with the lower bound between the Feigenbaum accumulation point ($\alpha = 1.401$ below which there is no chaos) and $2 \rightarrow 1$ band-merging point ($\alpha = 1.544$), and the upper bound near the maximum of $\alpha = 2.0$. The coupling strength ε was scanned from 0.5 to 0.9 with the lower bound such that remnant chaos is sufficiently suppressed and the upper bound near the maximum of 1.0, such that the local element still has

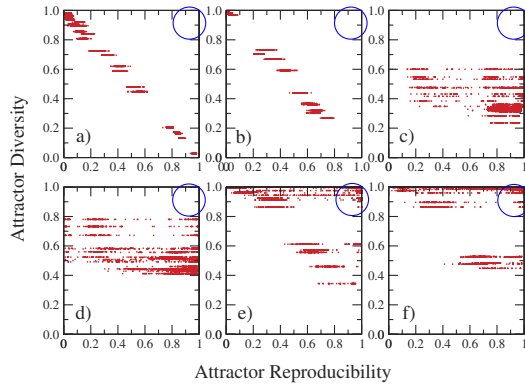


FIG. 2 (color online). Attractor diversity and reproducibility for various network topologies: (a) diffusive, (b) hierarchical, (c) small-world, (d) Watts-Strogatz, (e) scale-free, (f) ER-random. The system size was set to 50 nodes throughout except for the hierarchical network where it was set to 64. The number of simulations per part of a run was $M = 250$ and the transient time was 10^5 time steps. The blue circles denote the area of interest.

some effect. Therefore, with regards to attractor reproducibility and diversity, the scanned parameter region should basically cover the interesting parameter pairs.

While Fig. 2 shows the relationship between reproducibility and diversity, it does not provide a quantitative measure. To obtain that, the number of nodes was doubled and the condition for classifying attractors as identical was made more stringent by omitting the averaging over nodes with an identical number of links. For example, by setting $y_{i,r} = \sum_T x_n^i$ for run r . This results in the attractor diversity to be at or near its maximum. Then the reproducibility for the parameter region was scanned as in Fig. 2 and plotted in the histogram depicted in Fig. 3(a). The figure shows that the scale-free topology has the highest frequency of combining large diversity with large reproducibility. However, it can also be seen that ER-random networks appear to display this property to some degree.

As Fig. 3(a) combines all the runs of all the parameter pairs into a single figure, it is not clear how scale-free and random networks compare. For example, the scale-free data could stem from many parameter pairs and the ER-random data could be from a single pair. If so, one cannot conclude that the combination of large diversity with high reproducibility is more common in scale-free networks. In order to investigate this, for the parameter pair which yielded the highest reproducibility in Fig. 3(a) ($\alpha = 1.7$, $\epsilon = 0.9$ for both the scale-free and ER-random topology), the result of 1000 runs is depicted in Figs. 3(b) and 3(c). As can be seen, the number of high reproducibility attractors is much larger for scale-free networks than for ER-random networks. This is even more so when increasing the system size to $N_N = 200$ as depicted in Fig. 3(d). Consequently, in, e.g., an evolutionary process where reproducibility is of great importance, there should be a clear tendency towards, and thus a dynamical advantage of, the scale-free topology

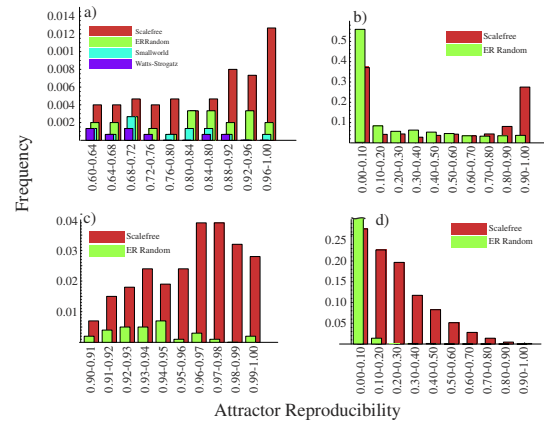


FIG. 3 (color online). (a) Histogram depicting attractor reproducibility of all the network topologies shown in Fig. 1 with the system size increased to $N_N = 100$. For the topologies of Fig. 1(a) and 1(b) none of the data falls within the plotted bin range. (b) Histogram of the attractor reproducibility of the scale-free and ER-random networks for the parameters in (a) that yield the highest reproducibility, $\alpha = 1.7$, $\epsilon = 0.9$, with the frequency determined from 1000 runs per topology. (c) Same as (b) with small bins in the high reproducibility region. (d) same as (b) but with the system size increased to $N_N = 200$ and the frequency determined from 1500 runs per topology.

if the underlying local dynamics can be represented by a simple chaotic map.

Next it is investigated whether the possibility of obtaining a large diversity combined with high reproducibility is limited to a small parameter region. As in Fig. 2, a region of parameter space is scanned, but this time the simulation only keeps track of whether the maximal reproducibility in 200 and 50 runs is larger than 0.99 (i.e., one or two different attractors). The outcome is plotted in Fig. 4 where the square corresponding to a parameter pair is plotted in yellow if the reproducibility is greater than 0.99 and blue otherwise. As can be seen, large reproducibility with large diversity is possible without fine tuning the parameters.

Attractors can graphically be visualized in node-amplitude plots where the value of a node is plotted versus

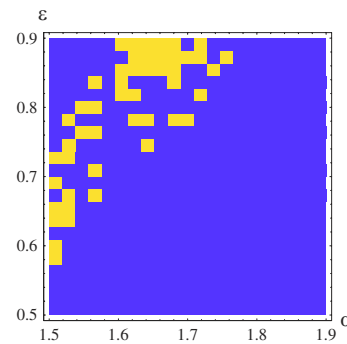


FIG. 4 (color online). Large reproducibility in the scale-free network versus α and ϵ . The yellow squares indicate a reproducibility greater than 0.99 while the blue squares indicate a reproducibility smaller or equal than 0.99. The number of nodes is $N_N = 100$.

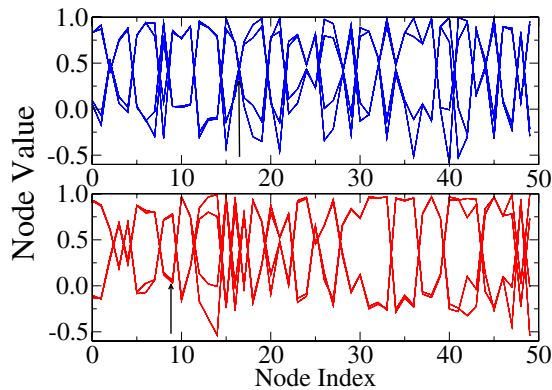


FIG. 5 (color online). Single-site switchable attractors. The top and bottom attractors can be switched by providing an input of -1 for a few times over a short period of time at the sites indicated by the arrows. The parameters were set to $\alpha = 1.7$ and $\varepsilon = 0.7$, and the system size was $N_N = 50$.

the index of the node. As can be inferred from Fig. 2, for a given scale-free topology, one, two, or more attractors can coexist. Two interesting attractors are shown in Fig. 5. In this case, the two attractors are the only two attractors, and when starting from random initial values for each of the nodes, the top attractor is reached roughly one third of the time and the bottom attractor two thirds of the time. A particularly interesting behavior of these attractors is that it is possible to switch between the two deterministically by applying input to *single* sites. This is reminiscent of mechanisms encountered in gene circuits [26,27] like, e.g., the toggle switch [28] or other combinatorial approaches [29] and has thus far not been observed in networks of chaotic nodes as described here. The sites that lead to attractor switching have an intermediate number of connections and an input at these sites will kick the system off one of the attractors but not the other. As there is some remnant chaos in the system, the effect of providing an input at a single time step may not permeate through the network and the system may fall back to the original attractor. However, when the input was applied a few times over a relatively short period of time, the attractor was always observed to switch in 100 trials. Although this type of switching does not appear to be present in the majority of the two-attractor scale-free networks, it was nevertheless common enough to consider it a distinct class of behavior.

Even though the hierarchical network is scale free, due to its given arrangement of nodes, there is no diversity in node arrangements. With regards to attractor diversity and reproducibility, the behavior is similar to that of the diffusive network. Hierarchical features and modularity, however, are concepts that may play important roles in certain networks like mass transfer in metabolism. It would therefore be interesting to see whether the addition of random links or the random rewiring of some percentage of the nodes would make it possible to recover attractor reproducibility.

In summary, a scale-free topology appears to not only have advantages that are direct consequences of how the

nodes are linked but also, for living systems, essential—advantages that are indirect consequences in that it structurally modifies the types of dynamics encountered. In an evolutionary process, it would seem that networks incapable of allowing for both structural variety (diversity) and controllable predetermined results (reproducibility) will be less fit. For the networks investigated here, the scale-free topology is the only topology which clearly displays these two properties and this may therefore provide a further reason as to why they are so common in biological systems.

This work is partially supported by NUS Grant No. WBS: R-144-000-138-112.

*Email address: willeboordse@yahoo.com

Electronic address: <http://www.willeboordse.ch/science/>

- [1] A.-L. Barabási and R. Albert, *Science* **286**, 509 (1999).
- [2] R. Albert and A.-L. Barabási, *Rev. Mod. Phys.* **74**, 47 (2002).
- [3] A.-L. Barabási and Z. Oltvai, *Nat. Genet.* **5**, 101 (2004).
- [4] S.H. Strogatz, *Nature (London)* **410**, 268 (2001).
- [5] I. Stewart, *Nature (London)* **427**, 601 (2004).
- [6] M. Argollo de Menezes and A.-L. Barabási, *Phys. Rev. Lett.* **92**, 028701 (2004).
- [7] A. Raval, *Phys. Rev. E* **68**, 066119 (2003).
- [8] M.E.J. Newman, *SIAM Rev.* **45**, 167 (2003).
- [9] D.J. Watts and S.H. Strogatz, *Nature (London)* **393**, 440 (1998).
- [10] A. Wagner and D.A. Fell, *Proc. R. Soc. B* **268**, 1803 (2001).
- [11] P. Erdős and A. Rényi, *Publ. Math. Inst. Hung. Acad. Sci.* **5**, 17 (1960).
- [12] E. Ravasz, A.L. Somera, D.A. Mongru, Z.N. Oltvai, and A.-L. Barabási, *Science* **297**, 1551 (2002).
- [13] K. Kaneko and T. Yomo, *J. Theor. Biol.* **199**, 243 (1999).
- [14] J.A. Shapiro, *J. Biol. Phys.* **28**, 745 (2002).
- [15] K. Kaneko, *Physica D (Amsterdam)* **41**, 137 (1990).
- [16] F.H. Willeboordse and K. Kaneko, *Phys. Rev. Lett.* **73**, 533 (1994).
- [17] F.H. Willeboordse, *Chaos* **13**, 533 (2003).
- [18] P.G. Lind, J. Corte-Real, and J.A.C. Gallas, *Phys. Rev. E* **69**, 026209 (2004).
- [19] T. Shibata, T. Chawanya, and K. Kaneko, *Phys. Rev. Lett.* **82**, 4424 (1999).
- [20] A. Crisanti, M. Falcioni, and A. Vulpiani, *Phys. Rev. Lett.* **76**, 612 (1996).
- [21] S. Manrubia and A. Mikhailov, *Europhys. Lett.* **53**, 451 (2001).
- [22] Z.N. Oltvai and A.-L. Barabási, *Science* **298**, 763 (2002).
- [23] F.H. Willeboordse, *Chaos Solitons Fractals* **2**, 609 (1992).
- [24] F.H. Willeboordse, *Phys. Rev. E* **47**, 1419 (1993).
- [25] R.M. May, *Nature (London)* **261**, 459 (1976).
- [26] J. Hasty, D. McMillen, and J.J. Collins, *Nature (London)* **420**, 224 (2002).
- [27] M.E. Wall, W.S. Hlavacek, and M.A. Savageau, *Nature Rev. Genet.* **5**, 34 (2004).
- [28] T.S. Gardner, C.R. Cantor, and J.J. Collins, *Nature (London)* **403**, 339 (2000).
- [29] C.C. Guet, M.B. Elowitz, W. Hsing, and S. Leibler, *Science* **296**, 1466 (2002).